Preprints.org

Article

Not peer-reviewed version

Retention of Tuning for Vibro-Impact and Linear Dampers Under Periodic Excitation

Petro Lizunov , Olga Pogorelova , Tetiana Postnikova *

Posted Date: 30 December 2025

doi: 10.20944/preprints202512.2637.v1

Keywords: vibro-impact; damper; nonlinear energy sink; tuned mass damper; efficiency; tuning

Preprints.org is a free multidisciplinary platform providing preprint service that is dedicated to making early versions of research outputs permanently available and citable. Preprints posted at Preprints.org appear in Web of Science, Crossref, Google Scholar, Scilit, Europe PMC.

Copyright: This open access article is published under a Creative Commons CC BY 4.0 license, which permit the free download, distribution, and reuse, provided that the author and preprint are cited in any reuse.

Preprints.org (www.preprints.org) | NOT PEER-REVIEWED | Posted: 30 December 2025 doi:10.20944/preprints202512.2637.v1

Disclaimer/Publisher's Note: The statements, opinions, and data contained in all publications are solely those of the individual author(s) and contributor(s) and not of MDPI and/or the editor(s). MDPI and/or the editor(s) disclaim responsibility for any injury to people or property resulting from any ideas, methods, instructions, or products referred to in the content.

Article

Retention of Tuning for Vibro-Impact and Linear Dampers Under Periodic Excitation †

Petro Lizunov [1], Olga Pogorelova [2] and Tetiana Postnikova [2]

[1] Department of Structural Mechanics, Kyiv National University of Construction and Architecture, 31 Povitryanykh Syl Ave., Kyiv, Ukraine, 03680

[2] Research Institute of Structural Mechanics, Kyiv National University of Construction and Architecture, 31 Povitryanykh Syl Ave., Kyiv, Ukraine, 03680

* Correspondence: posttan@ukr.net

† Presented at the 6th International Electronic Conference on Applied Sciences, Online, 9–11 December 2025.

Abstract

This work studies the ability of a single-sided vibro-impact nonlinear energy sink (SSVI NES) and a tuned mass damper (TMD) to maintain their vibration reduction performance when the natural frequency of the primary structure (PS), which is determined by its stiffness, changes. Both types of dampers demonstrate high efficiency in mitigating the PS vibrations under periodic excitation if their parameters are optimized at a specific PS natural frequency. Their ability to reduce PS vibrations changes similarly for both types of dampers when this structural parameter is changed.

Keywords: vibro-impact; damper; nonlinear energy sink; tuned mass damper; efficiency; tuning

1. Introduction

The problem of reducing unwanted vibrations in structures has been concern to engineers and scholars for many years. Various solutions have been found, ranging from vibration isolation [1] to vibration control devices that are coupled to the main structure and can be active, passive, and hybrid. Passive control devices that do not require additional energy sources can be linear, such as Tuned Mass Damper (TMD), and nonlinear, such as Nonlinear Energy Sink (NES). TMDs have been widely discussed in scientific literature and still being discussed today and have been implemented in engineering practice, particularly in several well-known structures. The papers [2,3] propose combining TMD with vibro-impact NES (VI NES). These comparative studies compare systems with TMD or VI NES and system with TMD+VI NES. Optimal parameters values can optimize the performance of the coupled system. The systems are subjected to harmonic excitation, but in [2] the system is also subjected to seismic excitation. NES with cubic stiffness was proposed long ago, back in [4], but it was widely discussed later, over the past two decades, within the framework of Targeted Energy Transfer (TET) theory. According to this theory, due to the system nonlinearity, NES takes part of the energy from the main structure and dissipates it. The shortcomings discovered in NESs encourage scientists to develop their new types. The limitations of energy threshold and insufficient robustness in NESs are noted in [5]. The authors also point out insufficient adaptability of conventional NES in complex engineering environments. Referring to [6], they note that conventional NES possesses certain limitations in practical applications. However, in their opinion, the damping performance and robustness of NES can be significantly improved by introducing asymmetric stiffness characteristics. Parallel asymmetric NESs with three repulsive magnets are studied numerically and experimentally in [7]. Parameter optimization is performed using a genetic algorithm GA. Different types of NESs are discussed in [8,9]. In a recent article [9], the authors propose a novel device that combines a traditional tristable NES with cubic nonlinear damping. The study presented in [10] investigates the efficiency of a double-sided vibro-impact nonlinear energy sink located in a cavity inside a linear oscillator. The efficiency is evaluated by the ratio of the energy

© 2025 by the author(s). Distributed under a Creative Commons CC BY license.

Preprints.org (www.preprints.org) | NOT PEER-REVIEWED | Posted: 30 December 2025 doi:10.20944/preprints202512.2637.v1

dissipated by the VI NES to the total energy of the system. The authors optimize the parameters using deterministic (by a genetic algorithm GA) and stochastic optimization methods.

This paper discusses the ability of single-sided vibro-impact NES (SSVI NES) and TMD to maintain their vibration reduction performance when the natural frequency of the primary structure changes. This phenomenon, when changing the damping of the primary structure and the external force intensity, was demonstrated in our previous paper [11]. The purpose of this work is to show that both SSVI NES and TMD demonstrate high efficiency in mitigating the PS vibrations if their parameters are optimized at a certain value of the PS natural frequency. Their efficiency for both damper types changes in a similar way with changes in this structural parameter.

2. Materials and Methods

A light damper (both SSVI NES and TMD) with mass m_2 is coupled to a heavy primary structure (PS) with mass m_1, which is a linear oscillator (Figure 1). The mass ratio $m_2/m_1 \cdot 100\ \% = 6\ \%$. Clearance C and initial distance D are optimized for SSVI NES, but selected with large values for TMD, which ensures the absence of impacts, i.e., the damper operates as linear.

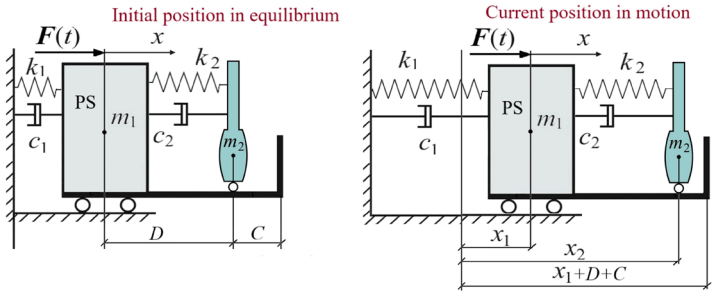

Figure 1. Conceptual scheme of a PS connected to a damper.

Harmonic exciting force $F(t) = P\,cos(\omega t)$ acts on the PS. The repeated impacts on the obstacle and on the PS directly that occur during SSVI NES motion are simulated using nonlinear Hertz's contact force according to his quasi-static contact theory [12]: $F_{con}(z) = K \cdot [z(t)]^{\frac{3}{2}}$, where $z(t)$ is the rapprochement of the colliding bodies during an impact. The Signorini's contact conditions are as follows:

$x_1 \geq x_2$, $\quad z_1 = x_1 - x_2$ for direct impacts on the PS,

$x_2 \geq x_1 + (D + C)$, $\quad z_2 = x_2 - x_1 - (D + C)$ for impacts on an obstacle.

Coefficient K characterizes the mechanical and geometrical characteristics of colliding surfaces and varies for different surfaces:

$$K_i = \frac{4}{3}\frac{q_i}{(\delta_i + \delta_{i+1})\sqrt{A_i + B_i}}, \quad \delta_i = \frac{1 - \nu_i^2}{\pi E_i}, \quad i = 1,3.$$

Here E_i and ν_i are the Young's moduli and Poisson's ratios of the four colliding surfaces; the constants A_i, B_i, and q_i are their joint geometrical characteristics, which are calculated according to the known table [12] depending on the type of contact surfaces. Assuming that both damper surfaces are spherical of large radii, PS and obstacle surfaces are flat, then $A_i = B_i = 1/2R_i$, where R_i is the large radius of the damper surfaces.

Combining the Signorini's contact conditions and the Hertz contact law, and using discontinuous Heaviside step function to "activate" the contact forces, we write down the motion equations for this system in accordance with the fundamental law of dynamics as follows:

$$\begin{aligned} m_1\ddot{x}_1 + c_1\dot{x}_1 + k_1x_1 - c_2(\dot{x}_2 - \dot{x}_1) - k_2(x_2 - x_1 - D) \\ = F(t) - H(z_1)F_{con}(z_1) + H(z_2)F_{con}(z_2), \\ m_2\ddot{x}_2 + c_2(\dot{x}_2 - \dot{x}_1) + k_2(x_2 - x_1 - D) = H(z_1)F_{con}(z_1) - H(z_2)F_{con}(z_2). \end{aligned} \quad (1)$$

The initial conditions are:

© 2025 by the author(s). Distributed under a Creative Commons CC BY license.

Preprints.org (www.preprints.org) | NOT PEER-REVIEWED | Posted: 30 December 2025 doi:10.20944/preprints202512.2637.v1

$x_1(0) = 0,\ x_2(0) = D,\ \dot{x}_1(0) = \dot{x}_2(0) = 0.$

To solve the Cauchy problem, this stiff set of ordinary differential equations is integrated using the stiff solver *ode23s* from the *Matlab* platform, which provides a variable integration step and makes it extremely small at the impact points.

The dynamics of a system with a linear tuned mass damper is described by the same equations if there are no contact forces, which is determined by the zero values of the Heaviside function. Large values of the clearance C and initial distance D ensure its zero values and, consequently, the absence of contact forces.

The dampers are designed to mitigate the PS vibrations, i.e., to reduce its mechanical energy, which is calculated by the well-known formula, where x_1(t) and $\dot{x}_1$(t) are the results of integration of the motion equations: $E_{1total}(t) = E_{1kinetic}(t) + E_{1poten}(t) = \frac{m_1\dot{x}_1(t)^2 + k_1x_1(t)^2}{2}$. The energy of the damper is: $E_2(t) = \frac{m_2\dot{x}_2(t)^2 + k_2(x_2(t) - D)^2}{2}$.

The system parameters are as follows: m_1=1000 kg, m_2=60 kg, c_1=452 N·s/m, P=800 N.

Mechanical characteristics of PS and obstacle surfaces are as follows: $E_1 = E_3 = 2.1 \cdot 10^{11}$ N/m², $\nu_1 = \nu_3 = 0.3$.

Mechanical characteristics of damper surfaces are as follows: $E_2 = 2.21 \cdot 10^7$ N/m², $E_4 = 2.05 \cdot 10^7$ N/m², $\nu_2 = \nu_4 = 0.4$. The PS natural frequency, determined in our case by the PS stiffness, changes when the PS stiffness changes: $\omega_0 = \sqrt{k_1/m_1}$.

The optimal damper parameters were found using *Matlab* platform tools. The maximum PS energy is selected as the objective function. First, their approximate values for certain value of the PS stiffness were determined using the *surf* program (Figure 2).

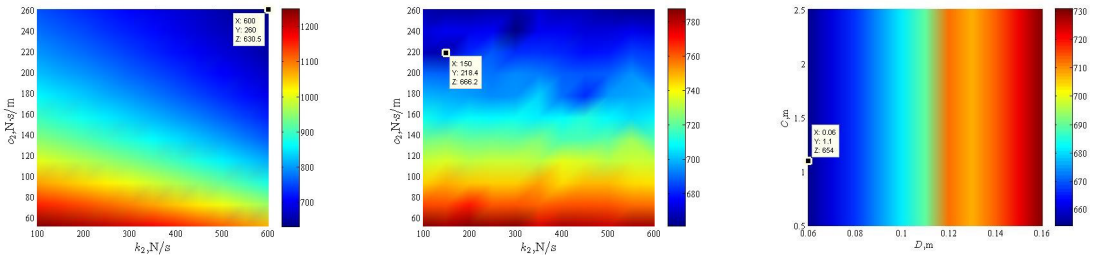

(**a**) (**b**) (**c**)

Figure 2. Finding the optimal parameters of linear TMD and SSVI NES with mass ratio m_2/m_1 of 6% coupled to PS with stiffness $k_1 = 3.95 \cdot 10^4$ N/m using the *surf* program.

Then, the parameters values taken from the Data Tip were refined using the *fminsearch* program (Table 1).

Table 1. Fragment generated by the *fminsearch* program during optimization of SSVI NES parameters.

$k_{2\ opt}$, N/m	$c_{2\ opt}$, N·s/m	D_{opt}, m	C_{opt}, m	$E_{1\ max}$, J
1.500000E+002	*2.184000E+002*	*6.000000E-002*	*1.100000E-001*	*6.662000E+002*
2.100000E+002	*2.184000E+002*	*6.000000E-002*	*1.100000E-001*	*6.611376E+002*
2.203750E+002	*2.334500E+002*	*6.037500E-002*	*3.622500E-001*	*5.731080E+002*
⋮	⋮	⋮	⋮	⋮
2.150000E+002	*2.320000E+002*	*6.000000E-002*	*3.600000E-001*	*5.630000E+002*

3. Results and Discussion

The damper parameters after performing the optimization procedures are presented in Table 2.

© 2025 by the author(s). Distributed under a Creative Commons CC BY license.

Preprints.org (www.preprints.org) | NOT PEER-REVIEWED | Posted: 30 December 2025 doi:10.20944/preprints202512.2637.v1

Table 2. The optimized parameter values for the SSVI NES and TMD with mass ratio m_2/m_1 of 6% coupled to PS with stiffness k_1=3.95·10^4N/m.

Damper type	m_2, kg	k_2, N/m	c_2, N·s/m	D, m	C, m
SSVI NES	60	215	232	0.06	0.36
TMD	60	600	262	2.08	4.7

The dampers with these optimized parameters ensure their high efficiency in mitigating the PS vibrations, i.e., they effectively reduce its maximum energy. However, having an optimal design found for PS stiffness k_1=3.95·10^4 N/m, they change their performance when PS stiffness changes. The maximum energy behavior for the PS without a damper and PS coupled to the SSVI NES and TMD with optimized parameters when changing the PS stiffness k_1 is shown in Figure 3.

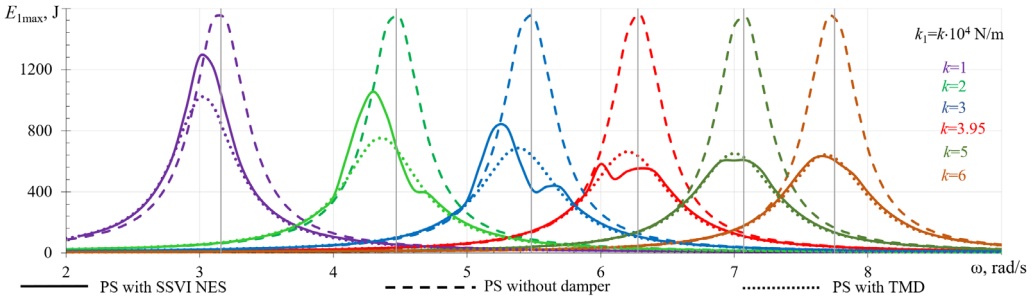

Figure 3. The reduction of maximum PS energy with attached SSVI NES and TMD tuned to k_1=3.95·10^4 N/m when changing the PS stiffness k_1.

In the version corresponding to the tuning shown in red, the oscillation suppression is achieved best. The SSVI NES provides two resonant peaks and reduces the PS vibrations in the resonance zone somewhat better than TMD. The mitigation is quite good for both the SSVI NES and the TMD at different PS stiffness values. Both damper types retain their tuning, but the TMD retains it somewhat better. With increasing the PS stiffness k_1 the energy reduction remains virtually unchanged and identical for SSVI NES and TMD. When PS stiffness decreases, the energy reduction worsens; moreover, this deterioration is greater for SSVI NES than for TMD. The resonance peak shifts to the left towards low frequencies. However, the energy reduction is maintained even at significantly low stiffness value. Figure 4 demonstrates the areas of bilateral SSVI NES impacts on the PS directly and on the obstacle in pink, as well as areas of unilateral impacts only on the PS in blue, where there are no impacts on the obstacle. These graphs also show the E_{1max} curves for PS without dampers, with SSVI NES and TMD attached, as well as the damper energy E_{2max} for SSVI NES. The vertical black lines indicate the resonance frequency.

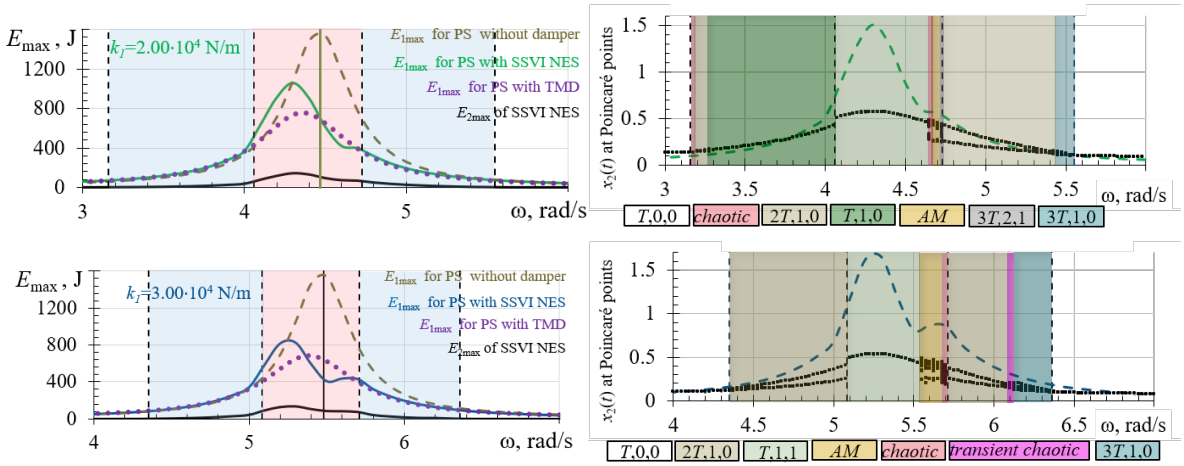

© 2025 by the author(s). Distributed under a Creative Commons CC BY license.

Preprints.org (www.preprints.org) | NOT PEER-REVIEWED | Posted: 30 December 2025 doi:10.20944/preprints202512.2637.v1

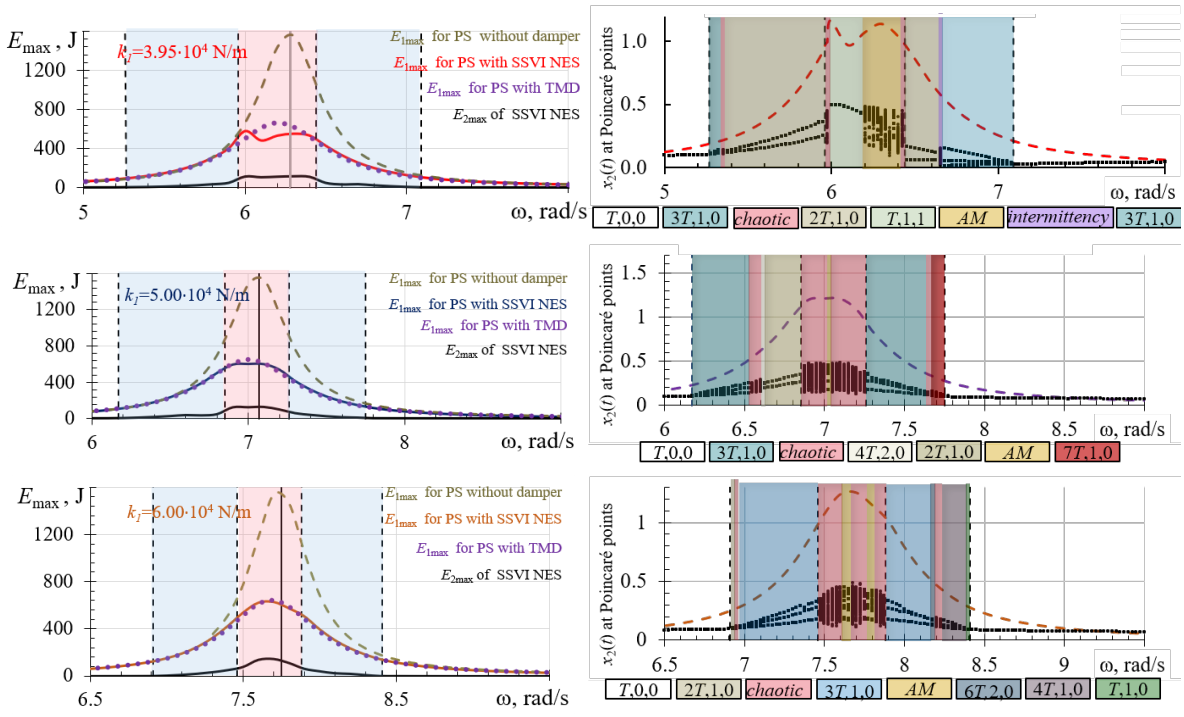

Figure 4. Graphs for five different values of PS stiffness k_1. Left: The zones of SSVI NES bilateral impacts in pink and unilateral impacts on the PS only in blue. The maximum energy of PS without damper, with SSVI NES and TMD attached, and the maximum damper energy. Right: Bifurcation diagrams of the system with SSVI NES attached.

Bifurcation diagrams in Figure 4 demonstrate rich complex dynamics of the system with SSVI NES attached. The maximum energy of the PS with SSVI NES attached is shown as a dotted curve for clarity. The following notation is used here: nT,m,k regime is a mode with periodicity nT, where T is the period of the exciting force; m is the number of direct damper impacts on the PS per cycle; k is the number of damper impacts on the obstacle per cycle. The system dynamics differs for different k_1, but in all five graphs, the periodic regimes with different periodicity and different numbers of impacts alternate with various irregular regimes – chaotic, amplitude-modulated (AM), and intermittent. Some of them are shown below in Figure 7.

To clarify the energy transfer process between the PS and the damper, the energy ratios are calculated as follows $R_1 = \frac{E_{1max}}{E_{1max}+E_{2max}}$ and $R_2 = \frac{E_{2max}}{E_{1max}+E_{2max}}$ [5]. These ratio values for different PS stiffness values k_1 are presented in Figure 5a. Figures 5b, c show the changes in these ratios as a function of the exciting force frequency ω for two k_1 values.

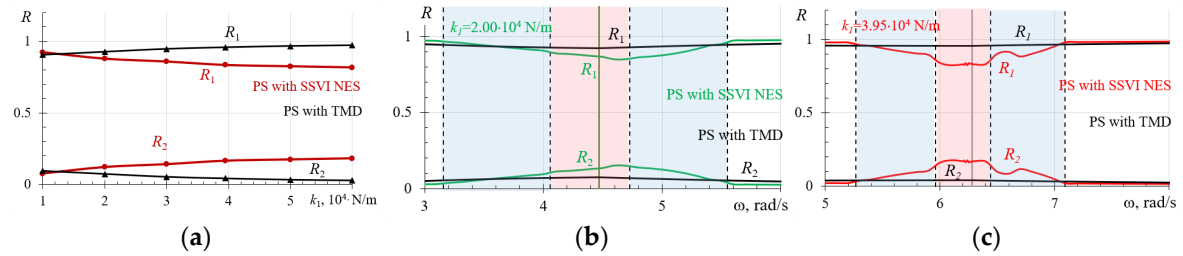

Figure 5. The energy ratios R_1 and R_2: (**a**) for different PS stiffness value k_1; (**b**) depending on exciting force ω for k_1=2.00·10⁴ N/m; (**c**) depending on exciting force ω for k_1=3.95·10⁴ N/m.

These graphs show that SSVI NES realizes the energy transfer from PS to damper somewhat better than TMD. Figure 6 shows the change in PS energy $E_1(t)$ and the damper energy $E_2(t)$ over time at resonance for PS without a damper and coupled to SSVI NES and TMD.

© 2025 by the author(s). Distributed under a Creative Commons CC BY license.

Preprints.org (www.preprints.org) | NOT PEER-REVIEWED | Posted: 30 December 2025 doi:10.20944/preprints202512.2637.v1

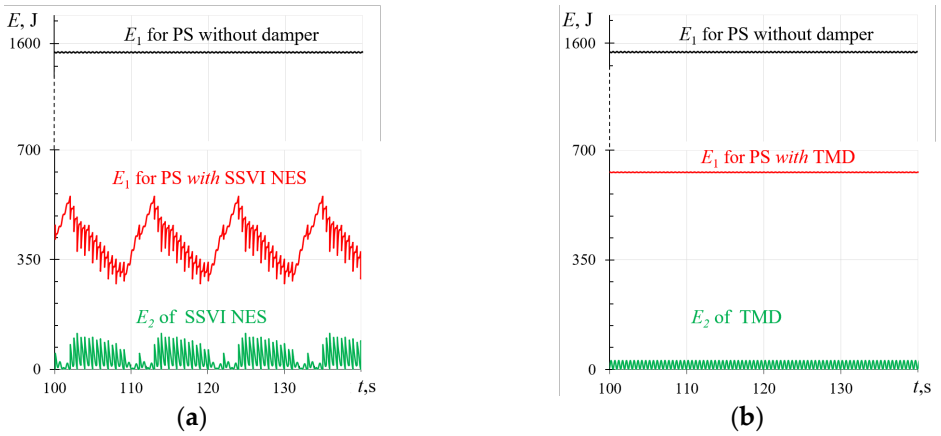

Figure 6. The PS energy $E_1(t)$ and the damper energy $E_2(t)$ as the functions of time at exciting force frequency ω =6.28 rad/s when PS with stiffness k_1=3.95·10⁴ N/m is coupled with dampers: (**a**) SSVI NES, (**b**) TMD.

The richness of the complex dynamics of the system with the SSVI NES connected is characterized by various irregular modes. Some of them are shown in Figure 7. These graphs show the damper displacements $x_2(t)$, the phase trajectories characteristic for each movement, the contact forces during damper direct impacts on the PS F_{conL} in blue, and the contact forces during damper impacts on the obstacle F_{conR} in green at different exciting force frequencies ω ,when the PS stiffness also varies.

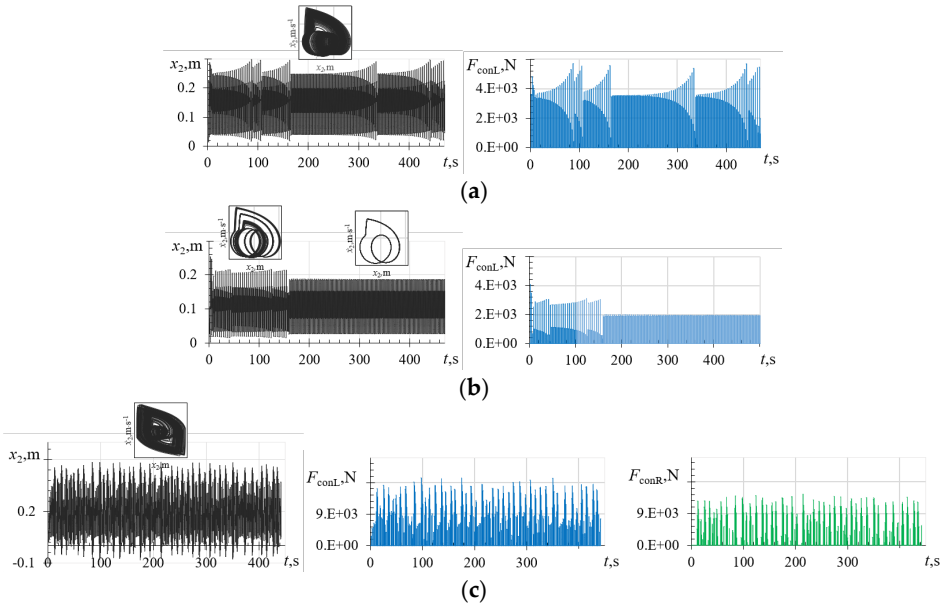

Figure 7. (**a**) Intermittency with unilateral impacts at ω=6.65 rad/s when PS stiffness k_1=3.95·10⁴ N/m. (**b**) Transient chaos with unilateral impacts at ω=6.10 rad/s when PS stiffness k_1=3.00·10⁴ N/m. (**c**) Chaotic motion with bilateral impacts at ω=7.10 rad/s when PS stiffness k_1=5.00·10⁴ N/m.

4. Conclusions

This study examined the ability of SSVI NES and TMD to maintain their reduction performance for PS under harmonic excitation when its stiffness changes. The study showed that both SSVI NES and TMD exhibit high efficiency in mitigating PS vibrations if their parameters are optimized at certain structural parameters values. They maintain their vibration reduction performance when the PS stiffness increases, but the PS energy reduction worsens when PS stiffness decreases. The deterioration in PS energy reduction is similar for both damper types, but the deterioration in reduction when using SSVI NES is slightly greater than when using TMD, i.e., TMD maintains its

© 2025 by the author(s). Distributed under a Creative Commons CC BY license.

Preprints.org (www.preprints.org) | NOT PEER-REVIEWED | Posted: 30 December 2025 doi:10.20944/preprints202512.2637.v1

tuning a bit better. At the same time, SSVI NES is slightly better than TMD at the transferring energy from the PS to the damper.

Author Contributions: All authors contributed equally to this work. All authors have read and agreed to the published version of the manuscript.

Funding: This research received no external funding.

Institutional Review Board Statement: Not applicable.

Informed Consent Statement: Not applicable.

Data Availability Statement: All the main data are contained in the article.

Conflicts of Interest: The authors declare no conflicts of interest.

References

1. Wu, S.; Yan, M.; Zhang, L.; Feng, L.; Yang, N. Nonlinear dynamic response of piecewise nonsmooth vibration isolation systems under base excitation. *J. Sound Vib.* 2026, 624, 119521. https://doi.org/10.1016/j.jsv.2025.119521
2. Di Egidio, A.; Briseghella, B.; Contento, A. Combined tuned mass damper and vibro-impacting nonlinear energy sink for the seismic protection of frame structures. *Structures* **2024**, 70, 107576.
3. Abdillahi, A.; Malekzadeh, M. Synergistic damping: Optimizing vibration control with TMDI and VI-NES integration in nonlinear systems. SSRN 2024, preprint. https://doi.org/10.2139/ssrn.4906091
4. Roberson, R.E. Synthesis of a nonlinear dynamic vibration absorber. *J. Franklin Inst.* 1952, 254, 205–220. https://doi.org/10.1016/0016-0032(52)90457-2
5. Qi, X.; Zhang, J.; Wang, J. Dynamics and vibration reduction performance of an asymmetric nonlinear energy sink inspired by skeletal muscle mechanisms. *J. Sound Vib.* 2026, 624, 119523. https://doi.org/10.1016/j.jsv.2025.119523
6. Zeng, Y.; Ding, H.; Du, R.-H.; Chen, L.-Q. Micro-amplitude vibration suppression of a bistable nonlinear energy sink constructed by a buckling beam. *Nonlinear Dyn.* 2022, 108, 3185–3207. https://doi.org/10.1007/s11071-022-07378-7
7. Guo, M.; Wu, Y.; Hu, C.; Tang, L.; Liu, K. Vibration suppression performance of tunable parallel asymmetric nonlinear energy sinks with distinct stability characteristics under impulse excitation. *J. Sound Vib.* 2025, 119537. https://doi.org/10.1016/j.jsv.2025.119537
8. Fang, Y.; Ma, X.; Xia, X.; Yu, R.; Zhong, Y.; Zhang, Z. Dynamics-guided constrained optimization of a piezoelectric nonlinear energy sink for structural vibration control. Eng. Struct. 2026, 346, 121668. https://doi.org/10.1016/j.engstruct.2025.121668
9. Li, X.; Qin, Y.; Lin, X.; Wang, Z.; Wang, L.; Yan, Z.; Nie, X. Parameter optimization and vibration control of tristable nonlinear energy sink incorporating with linear and nonlinear damping under impact excitation. Int. J. Dyn. Control 2025, 13, 12. https://doi.org/10.1007/s40435-025-01942-w
10. Abdollahi, A.; Bab, S. Improving vibration suppression by applying stochastic optimization to a coil-contained vibro-impact nonlinear energy sink within a linear oscillator framework. *Appl. Math. Model.* 2026, 151, 116479. https://doi.org/10.1016/j.apm.2025.116479

© 2025 by the author(s). Distributed under a Creative Commons CC BY license.

Preprints.org (www.preprints.org) | NOT PEER-REVIEWED | Posted: 30 December 2025 doi:10.20944/preprints202512.2637.v1

11. Lizunov, P.; Pogorelova, O.; Postnikova, T. Tuning of vibro-impact nonlinear energy sinks under changing structural parameters. Part 1. *Strength Mater. Theory Struct.* 2025, 114, 11–22. https://doi.org/10.32347/2410-2547.2025.114.11-22
12. Goldsmith, W. *The Theory and Physical Behaviour of Colliding Solids*; Edward Arnold Publishers Ltd: London, 1960.

Disclaimer/Publisher's Note: The statements, opinions and data contained in all publications are solely those of the individual author(s) and contributor(s) and not of MDPI and/or the editor(s). MDPI and/or the editor(s) disclaim responsibility for any injury to people or property resulting from any ideas, methods, instructions or products referred to in the content.

© 2025 by the author(s). Distributed under a Creative Commons CC BY license.